Core Density Turbulence in the HSX Stellarator

C.B. Deng[1], D.L. Brower[1], D.T. Anderson[2], F.S.B. Anderson[2], A. Briesemeister[3], K. Likin[2]

[1] Department of Physics and Astronomy, University of California Los Angeles, Los Angeles, California 90095

[2] Department of Electrical and Computer Engineering, University of Wisconsin-Madison, Madison, Wisconsin 53706

[3] Oak Ridge National Laboratory, Oak Ridge, Tennessee 37831

Abstract

Broadband turbulent density fluctuations are explored in the helically symmetric stellarator experiment (HSX) by investigating changes related to plasma heating power and location. No fluctuation response is observed to occur with large changes in electron temperature and its gradient, thereby eliminating temperature gradient as a driving mechanism. Instead, measurements reveal that density turbulence varies inversely with electron density scale length. This response is consistent with density gradient drive as one might expect for trapped electron mode (TEM) turbulence. In general, the plasma stored energy and particle confinement are higher for discharges with reduced fluctuations in the plasma core. When the density fluctuation amplitude is reduced, increased plasma rotation is also evident suggesting a role is also being played by intrinsic plasma flow.

1. Introduction

The stellarator configuration has demonstrated significant progress as a potential future nuclear fusion reactor. An intrinsic limitation making the stellarator less appealing than tokamaks results from direct orbit loss due to asymmetry of confining magnetic fields which increases at lower collisionality. This unfavorable transport scaling has recently been greatly diminished by implementing a variety of optimization methods. The confinement and plasma parameters achieved in LHD and W7-AS, for example, are similar to those obtained in tokamaks [1, 2]. In addition, there is evidence that anomalous transport is also reduced under these conditions [3]. HSX (Helically Symmetric eXperiment) is the first of a new class of stellarators which is optimized to greatly diminish neoclassical transport by introducing quasi-symmetry along the helical direction (QHS). On HSX, measurements show neoclassical confinement has been significantly improved for QHS plasmas when compared to the conventional stellarator configuration and overall confinement under these conditions may be determined by fluctuation-induced anomalous transport [4]. Linear 3D gyrokinetic calculations [5, 6] have predicted that the anomalous electron thermal transport in the HSX stellarator may be caused by trapped-electron mode drift wave turbulence. Both theoretical and experimental studies on turbulence-induced transport for a stellarator with quasi-symmetry will provide important contributions to the goal of future fusion reactor development.

This paper reports on the first core density fluctuation measurements in the HSX stellarator where the response of broadband turbulence is explored by investigating changes related to plasma heating power and location. Density fluctuations, equilibrium kinetic profile gradients and plasma stored energy are explored for two specific cases; (1) QHS plasmas with on-axis and off-axis inboard heating, and (2) variations in electron cyclotron resonance heating (ECRH) power. Broadband turbulent density fluctuations are observed to increase with density gradient while exhibiting no sensitivity to the electron temperature gradient. Reduced fluctuation levels

correspond to plasmas with increased stored energy and global particle confinement while the global energy confinement is unchanged. Measurements show that increased rotation also correlates with reduced fluctuation levels and improved confinement suggesting intrinsic plasma flow is potentially playing an important role. In addition to improved neoclassical confinement, quasi-helically symmetric HSX plasmas lead to increased flow in the direction of symmetry.

The paper is organized as follows; in Section 2 there will be an introduction of the measurement techniques (fluctuations, kinetic profiles) employed and the HSX device, followed in Section 3, by a detailed description of the experimental results. Implications of these measurements and their correlation with plasma parallel flow, density gradient and stored energy will be discussed in Section 4 along with a summary of the results in Section 5.

2. HSX Device and Multichannel Interferometer System

HSX is an unique stellarator which can be configured with quasi-symmetry in magnetic field strength along the helical axis. In HSX, the major radius is R_o=1.2 m; average minor radius is <a>=0.15 m. For data presented herein, the magnetic field strength at the helical axis is B=1 Tesla while the plasma is both produced and heated by up to 100kW of ECRH from 28 GHz gyrotrons employing O-mode heating at the fundamental frequency. The ECRH power deposition varies with heating location, being reduced for off-axis resonance [6]. As the cyclotron resonance is moved away from the magnetic-axis, the electron temperature becomes less peaked and flattens within the radius of the peak ECRH absorption. The total plasma stored energy is measured using a diamagnetic loop.

The multichannel interferometer diagnostic on HSX has been successfully used to measure both the equilibrium density distribution and density fluctuations. The system is optimized to measure electron density fluctuations by utilizing both phase (conventional [7] and differential [8] interferometry) and amplitude (collective far-forward scattering [9]) techniques. Information on core and edge fluctuations can be extracted by comparing chords with different impact parameters (central and edge) or by direct use of the differential interferometer approach. Density fluctuations with frequency up to 300 kHz are measured. The system consists of 9 chords covering nearly the entire plasma cross section with chord spacing and width ~1.5 cm. The interferometer spatial coverage is shown in Fig. 1. Due to spatial averaging across/along the

probing beam, the maximum observable fluctuation wavenumber is $k_\perp < 2$ cm^{-1} (~π/1.5 cm^{-1}), where $k_\perp$ is perpendicular to the magnetic field. Both the interferometer and far-forward scattering measurements are line-integrated. By utilizing the differential interferometer technique, core localized measurements of density gradient fluctuations are possible [10]. This approach directly determines the phase difference between two adjacent chords thereby localizing the measured phase difference to the region where the line-integrals sample different plasmas, i.e., the core for chords with small impact parameter [10]. Details of this techniques can be found in [8, 10]. Spatial localization sufficient to discriminate core from edge fluctuations in HSX is achieved.

In HSX, plasma flow is measured using a charge exchange recombination spectroscopy (CHERS) system employing a 30 keV diagnostic neutral beam [11]. The electron temperature profile is measured by multi-point Thomson scattering [12].

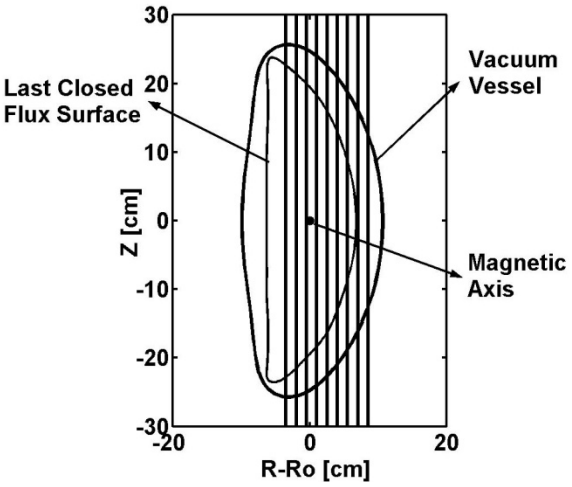

Figure 1. HSX vertical cut last closed flux surface and interferometer viewing chords.

3. Experimental Results

In order to gain insight into the nature of turbulence in the HSX stellarator, the relation between broadband turbulent density fluctuations, equilibrium profile gradients (density and electron temperature) and stored energy is studied for two specific cases; (1) QHS plasma with

on-axis and inboard heating, and (2) variations in ECRH power. In the following, each will be explored separately.

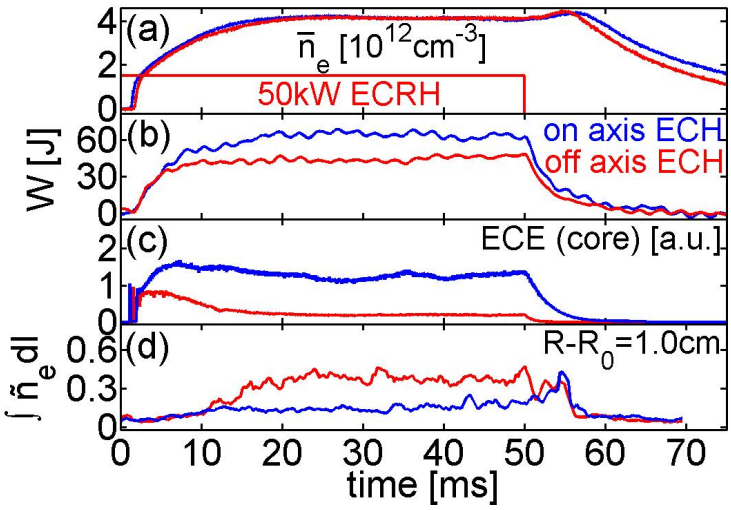

Figure 2. Plasma parameter evolutions for two QHS discharges: on-axis heating (blue), inboard HFS (r/a=-0.2) heating (red); (a) central line-averaged density, (b) plasma stored energy, (c) ECE in the plasma core, and (d) Line-integrated density fluctuations (R-R_o=1 cm) in the frequency range of 10-200 kHz. blue: on-axis and red: off-axis heating.

By slightly changing confining magnetic field strength, the heating location due to O-mode resonance at the fundamental frequency of the fixed-frequency 28 GHz gyrotron used for ECRH can be spatially displaced. A mean field B= 1 T at the magnetic axis is produced by a main coil current of 10.9 kA. By reducing the main coil current to 10.6 kA, the heating location is moved to r/a~0.2 on the high-field-side HFS (inboard at box-port location of interferometer system). Figure 2 shows the temporal evolutions of the basic plasma parameters for two discharges comparing on-axis and HFS heating. For each discharge, the plasmas were in the quasi-helically symmetric configuration with 50 kW of ECRH. The fueling gas was doped with methane (CH_4) in order to obtain sufficient signal for CHERS measurement. The line-averaged density was fixed at $4x10^{12}$ cm^{-3}, but the plasma stored energy reduced from 60J to 40J for the case of inboard heating. In addition, the ECE (electron cyclotron emission) signal at in the plasma core was substantially reduced for HFS heating. Line-integrated density fluctuations, as measured by interferometry for a central chord, increased by up to 100% for the discharge with HFS heating.

The density fluctuation frequency spectra from four interferometer chords with varying impact parameter ($x=R-R_o$) ranging from plasma center to edge are shown in Fig. 3. From these data one can readily distinguish that significant changes in the fluctuation amplitude are observed for the central chords (x=-0.5, 1.0 cm) while much smaller or no change occurs for chords further out (x=4.0 cm) when comparing on-axis and HFS heating. At the box-port location where these measurements are made, the last closed flux surface corresponds to x=6.8 cm. Experimentally determined differences are primarily in the frequency range from 20-120 kHz, which is between the electron collision frequency and bounce frequency for this study. Changes in the line-integrated density fluctuation profile over this frequency range are shown in Fig. 4. Despite the line-integrated nature of the measurements, one can infer that the fluctuation increase stems largely from the core plasma as the edge most chords are little changed. Based on measured profiles, these fluctuations correspond to $k_{\perp}\rho_s \le 0.8$ for plasma core and $k_{\perp}\rho_s \le 0.35$ near the edge, where $\rho_s \propto \sqrt{M_{ion}T_e}/B$

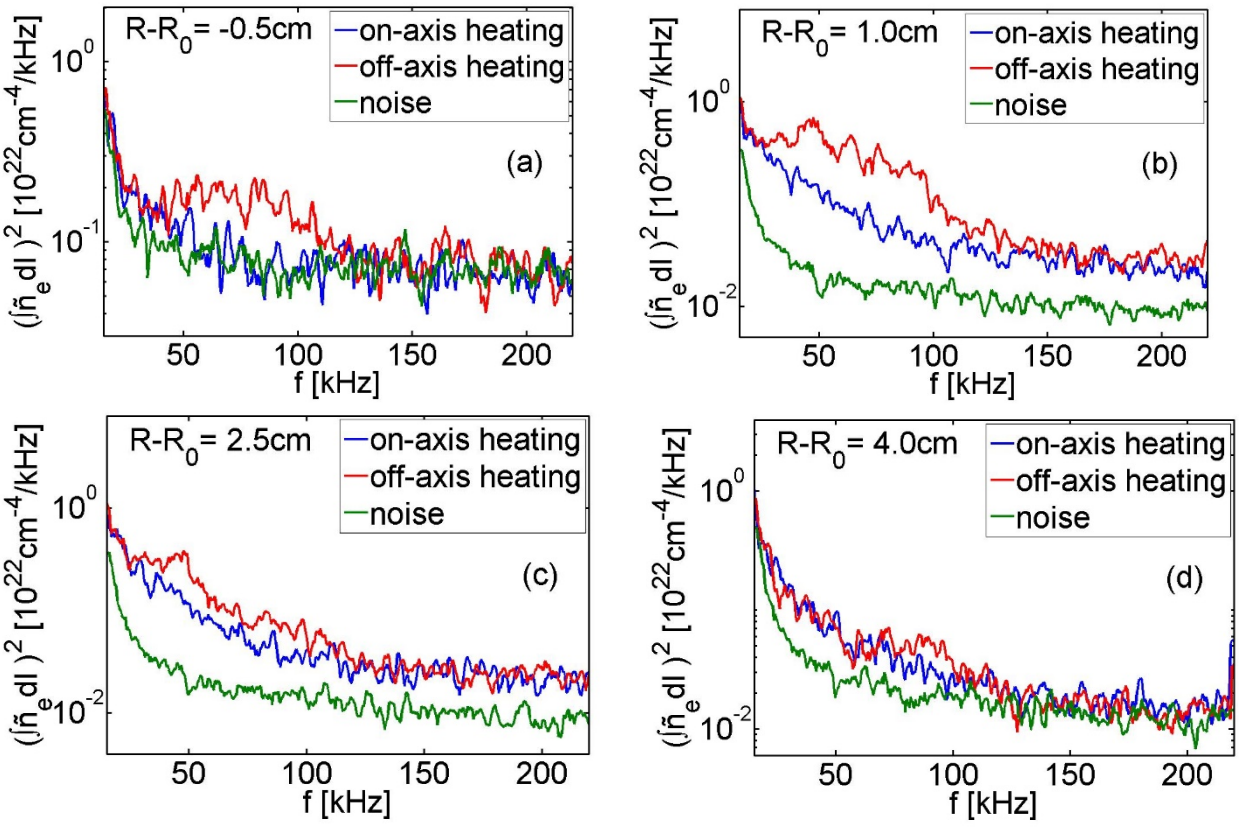

Figure 3. Frequency spectra of line-integrated density for different viewing chords. On-axis heating (blue) and HFS inboard heating (red). System noise level corresponds to the green trace.

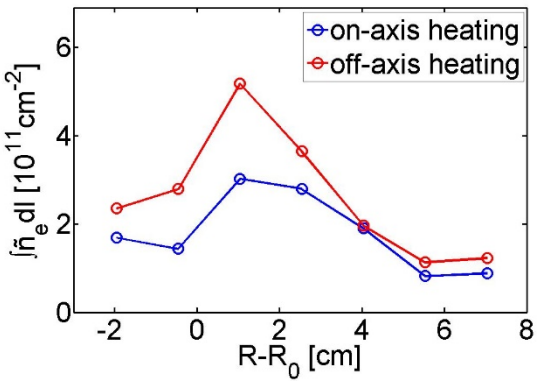

Figure 4. Line-integrated profile of density fluctuation amplitude in the 20-120 kHz frequency range for QHS plasma with on-axis (blue) and HFS heating (red).

To further explore the spatial distribution of the observed fluctuation increase, we employ the differential interferometry technique to measure core localized density gradient fluctuations. The results are shown in Fig. 5, for 3 differential chord pairs. Consistent with the line-integrated measurements of Figs. 3-4, the differential measurements using central chords show the largest change supporting the idea that the observed fluctuation increase is localized to the high-temperature plasma interior, and not the edge.

While care was taken to ensure the central line-integrated density is the same for the two plasmas being investigated, the electron temperature profiles are very different as the off-axis HFS heating leads to a much lower electron temperature, as shown in Fig. 6(a). We also note that the density profile and density gradients appear little changed (Fig. 6(b)) when compared to the peak electron temperature which falls from ~1.65 keV to 0.66 keV for the HFS heating case. Electron temperature for r/a>0.3 is little changed. Interestingly, for the HFS heating case, where the core electron temperature is much lower, along with the electron temperature gradients, the observed density fluctuation levels are significantly higher. This strongly suggests that the electron temperature gradient is not playing a role in driving the observed turbulence. In addition, ions are much colder than electrons in HSX and generally little affected by the ECRH. The ion temperature estimated from CHERS system is less than 100 eV, and with parabola-like profile. While T_e increases with ECRH power, T_i is relatively unchanged. The electron temperature profile for on-axis heating case is sufficiently peaked that the neoclassical thermo-diffusive flux may cause the density profile to be slightly hollow. The electron temperature can

be altered by changing either the heating power or location. In addition, experiments show that it is also possible to increase T_e by doping the fueling gas with methane. Figure 7 shows density gradient fluctuations and density profiles for different ECRH power levels and fueling gases for on-axis and off-axis heating. One can clearly see that the density fluctuation levels decrease with increased T_e (and T_e gradient), while the density gradients at r/a<0.5 are reduced, especially for HFS ECRH cases. In all cases tested, T_e and its gradient do not appear to be playing a role in driving the turbulent density fluctuations.

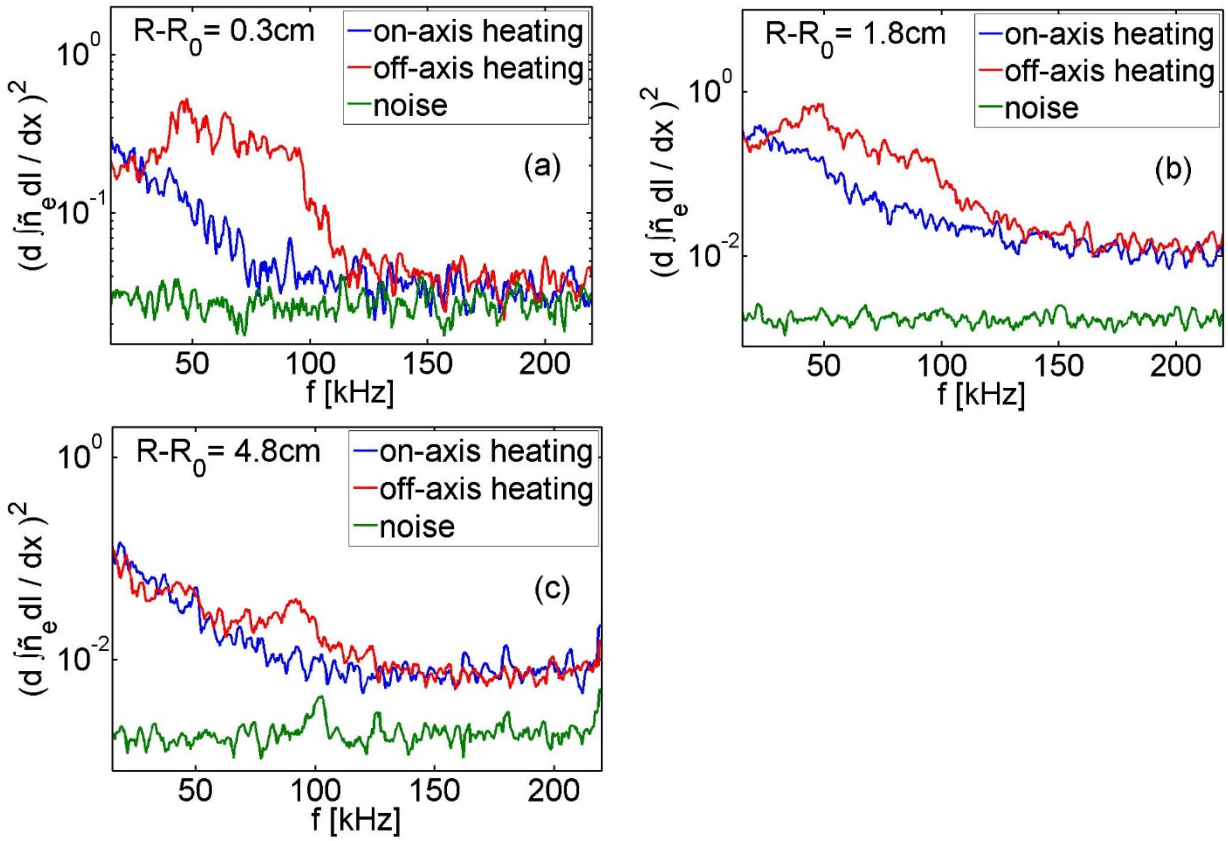

Figure 5. Frequency spectra of line-integrated density gradient fluctuations measured by differential interferometry. On-axis heating (blue) and HFS inboard heating (red). System noise level corresponds to the green trace.

Measured interior density fluctuations appear at least qualitatively consistent with core density gradient drive, i.e., fluctuations reduced with decreasing density gradient. In addition, the largest stored energy is observed to correlate with plasmas having the lowest density fluctuation levels. These claims are further supported by the data in Fig. 8. Here, the normalized, line-integrated density fluctuation amplitude for a central chord positioned at $R-R_o$=1cm is plotted

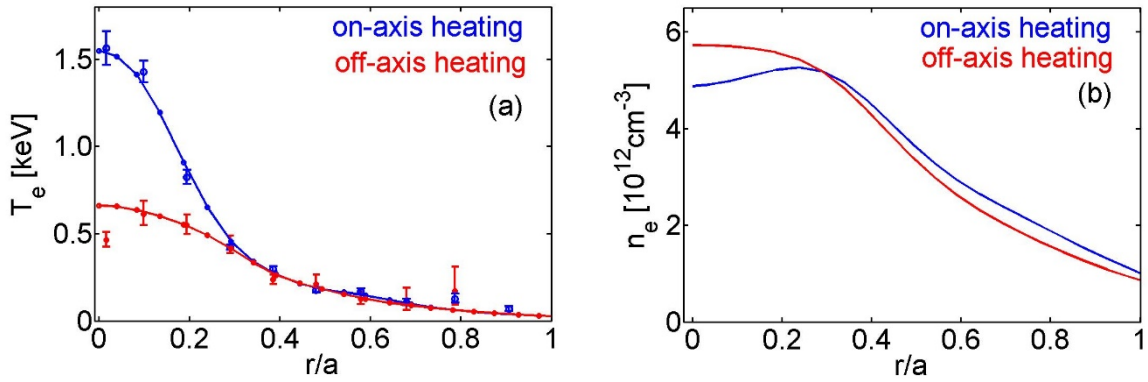

Figure 6. (a) Thomson scattering measurement of electron temperature, and (b) interferometric measurement electron density profiles in HSX. On-axis heating (blue) and HFS heating (red).

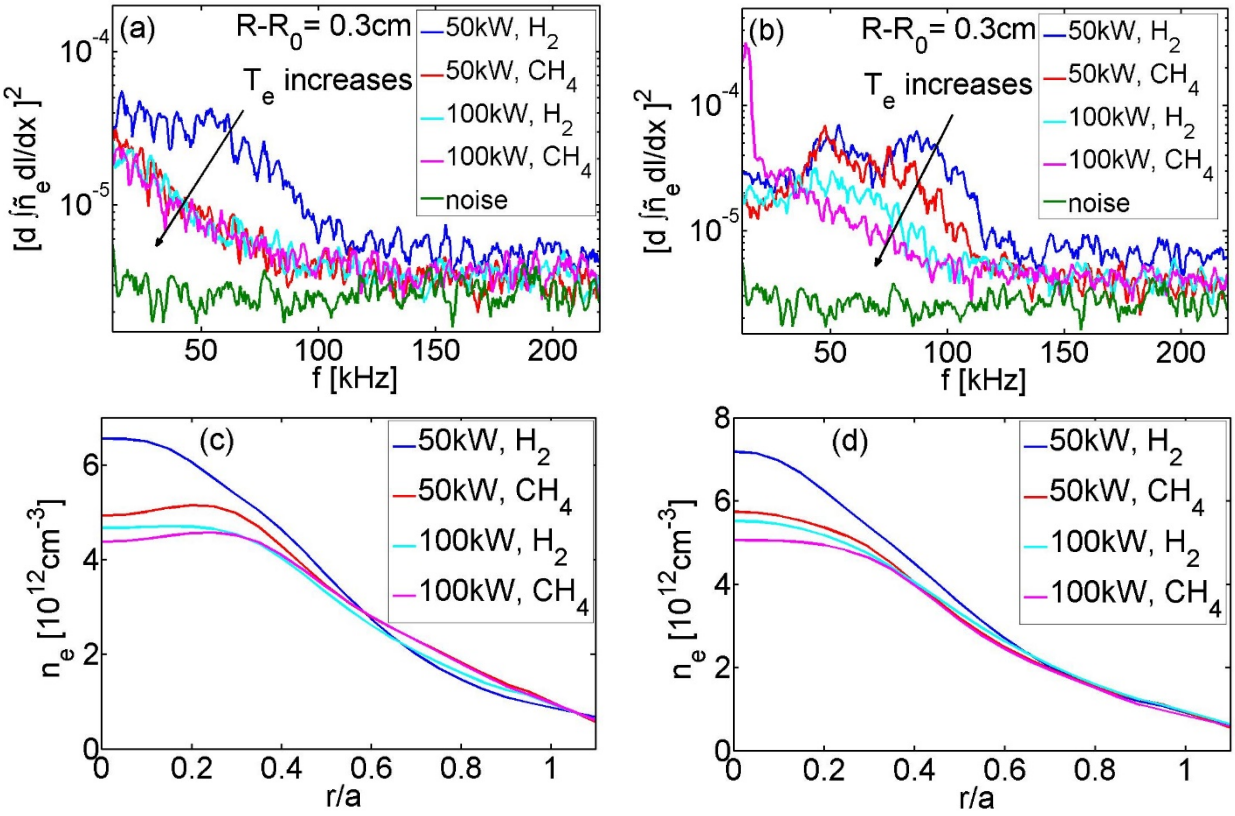

Figure 7. Core density gradient fluctuations at different electron temperatures, for plasmas heated at (a) magnetic axis, and (b) high field side for different ECRH power and fueling gases; (c) and (d) are density profiles for cases in (a) and (b). System noise level corresponds to the green trace.

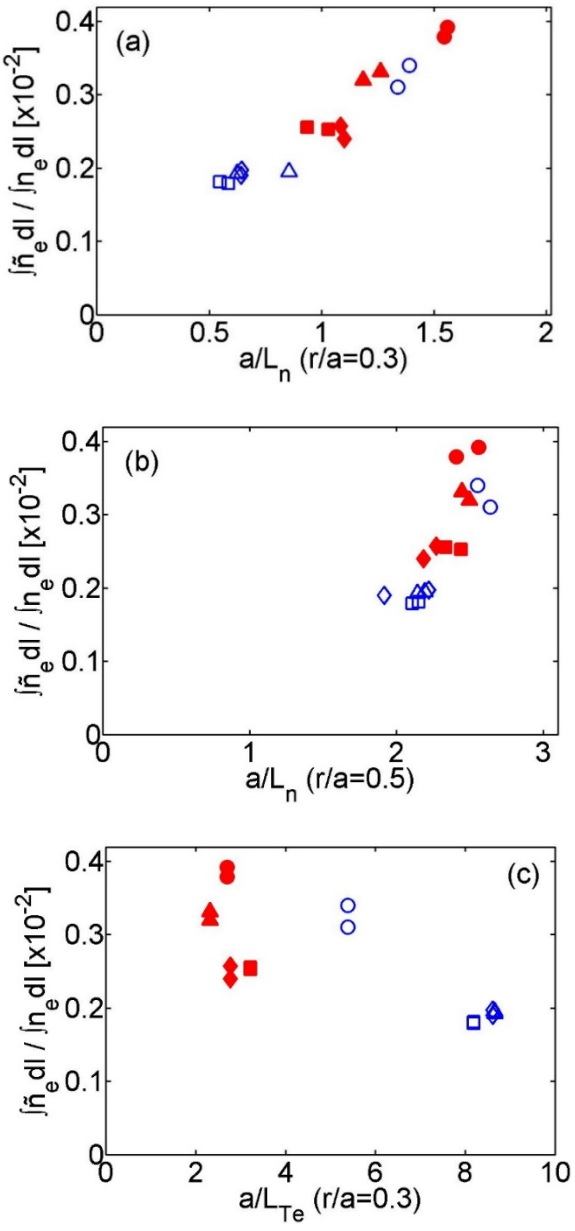

Figure 8. Normalized density fluctuations for central chord versus normalized inverse electron density gradient at positions (a) r/a=0.3 and (b) r/a=0.5, and (c) versus normalized inverse electron temperature at r/a=0.3. Symbols: open circle: 50kW on-axis ECH, H_2 fueling, open triangle: 50kW on-axis ECH, CH_4 fueling, open diamond 100kW on-axis ECH, H_2 fueling, open square: 100kW on-axis ECH, CH_4 fueling. Solid (red) symbols are for similar conditions to corresponding open (blue) symbols except heating is off-axis (HFS).

versus the normalized inverse density scalelength, $L_{ne}^{-1} = (dn_e/dr)/n_e$ (normalized to minor radius, a). The fluctuation amplitude is integrated over the frequency range from 20 to 120 kHz. From this plot we clearly see that the density fluctuation amplitude increases with reduced density scalelength, evaluated at both at r/a=0.3 and 0.5. Recall from earlier discussion and Figs. 3-5, that the fluctuations measured by the central chord are representative of the plasma interior. The edge density gradient is unchanged. As discussed earlier and shown in Fig. 8(c), plasma density turbulence levels show no evidence for electron temperature gradient drive.

On HSX, plasmas at similar density but higher temperature correspond to plasmas with increased stored energy. From Fig. 9(a), one can see that the measured density fluctuation level is reduced with increasing plasma stored energy. In addition to stored energy, the energy confinement time τ_E ($=W_{dia}/P_{abs}$, where P_{abs} is the absorbed ECRH power) can be estimated using measurements from diamagnetic flux loops. As shown in Fig. 9(b), there is no evidence for a change in the energy confinement time with density fluctuation amplitude. However, the energy confinement time is much more difficult to estimate and the errors are larger as determining the ECRH absorbed power is challenging. For fusion plasmas, global particle confinement can be estimated from the ratio of total number of particles (N) to particle source (S). We take the particle source as being approximately proportional to the intensity of H_α emission while the total number of particles is measured by interferometry. Changes in this ratio provide a proxy for changes in global particle confinement and can be compared with measured turbulence levels for cases examined in Fig. 8. Determining the absolute value of the global particle confinement is more complicated as it involves the calibrated absolute intensity of H_α emission over the plasma volume and 3D neutral gas modeling using a particle source code, e.g. DEGAS [4]. However, to determine the trend, we simple take the ratio, N/H_α. As shown in Fig. 9(c), there is evidence for particle confinement deterioration with density fluctuations as the ratio N/H_α falls with increased turbulence. We also note that the ratio N/H_α drops with increasing ECRH power.

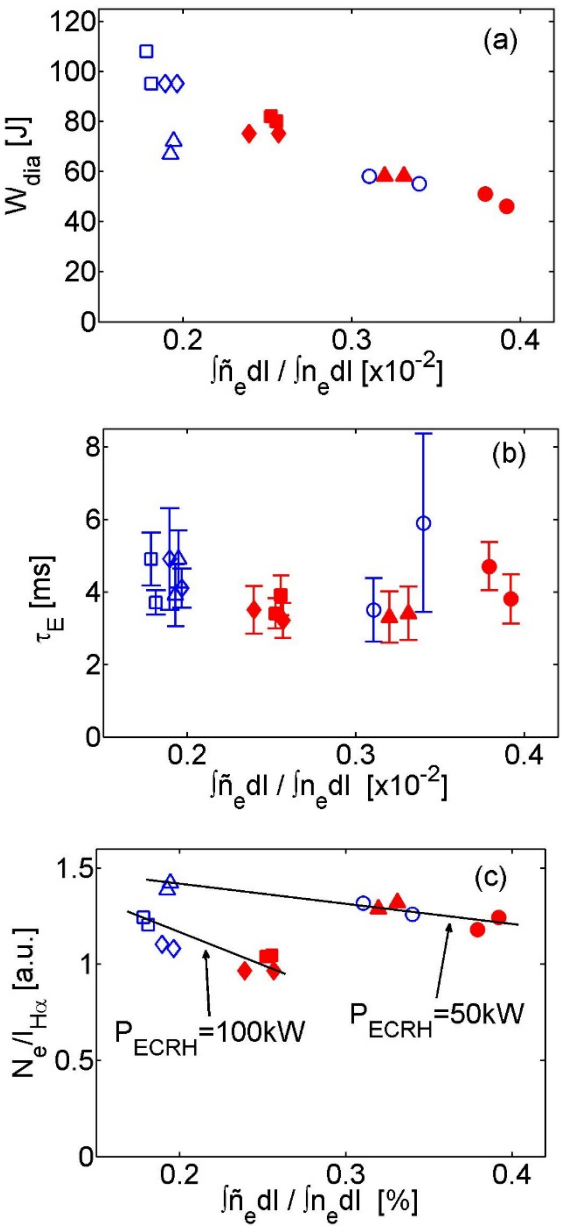

Figure 9. (a) Scaling of plasma stored energy with normalized density fluctuations for central chord. (b) Energy confinement time scaling with normalized density fluctuations from central chord. **(**c) Ratio of total particle number (N) to intensity of Hα emission ($I_{H\alpha}$) changes with normalized density fluctuations from central chord. Ratio is proportional to the global particle confinement time. Symbols: open circle: 50kW on-axis ECH, H_2 fueling, open triangle: 50kW on-axis ECH, CH_4 fueling, open diamond 100kW on-axis ECH, H_2 fueling, open square: 100kW on-axis ECH, CH_4 fueling. Solid (red) symbols are for similar conditions to corresponding open (blue) symbols except heating is off-axis (HFS).

4. Discussion of Experimental Results.

In the preceding section, changes in broadband turbulent density fluctuations, equilibrium density and electron temperature gradient, and global confinement were explored when comparing heating power levels and location (on-axis and off-axis) in QHS plasmas. In general, the measured turbulence showed an increase (decrease) with increasing (decreasing) density gradient as one might expect for a density gradient drive. However, no fluctuation response was observed to occur with large changes in electron temperature and its gradient, thereby eliminating the temperature gradient as a driving mechanism. These broadband fluctuations were measured in the frequency range 20-120 kHz (laboratory frame of reference) and correspond to $k_{\perp}\rho_s \leq 0.8$ for plasma core, $k_{\perp}\rho_s \leq 0.35$ near the edge. In addition, the plasma stored energy and global particle confinement were observed to increase for plasmas with reduced fluctuation levels while the global energy confinement was unchanged.

When the heating location of the QHS plasmas is moved or ECRH power changed, clear modifications in core density fluctuation amplitude and stored energy are noted. A plasma parameter not previously discussed for these HSX plasmas is the intrinsic plasma flow. In Fig. 10, we show the parallel flow for QHS plasmas with varying heating power and location. For the case of varying heating location, the plasma flow is significantly larger for on-axis as opposed to off-axis (HFS) ECRH. The observed flow increases from <5 to 10-15 km/s for on-axis heating in the plasma core. Recall, the core fluctuations and density gradient are both reduced while the temperature gradient increases significantly. In addition, the plasma flow is observed to increase with higher heating power on-axis while the density gradient and fluctuations are observed to decrease. For cases of varied heating location and power, the higher frequency fluctuations are observed for plasma exhibiting reduced flow thereby eliminating the possibility of a frequency shift, due to the Doppler Effect, producing the observed frequency change. In addition, global particle confinement is improved for the cases with increased flow for the same injected ECRH power.

Recent experimental results from HSX show that for QHS plasmas, the neoclassical transport is comparable to that in a tokamak and turbulent transport dominates throughout the plasma cross section. However, HSX is not optimized for anomalous transport associated with microturbulence. Recently, linear gyrokinetic calculations using the GENE code demonstrated

that the Trapped Electron Mode (TEM) is the dominant long-wavelength microturbulence instability across the majority of the HSX minor radius and the TEM is primarily driven by the electron density gradient for $a/L_n \geq 2.5$ [6]. The gradient of ion temperature is so low that the possibility of ITG mode is not considered for HSX. Simulations predict TEM density turbulence and maximum growth rates in the range $k_\perp \rho_s \leq 1$. In HSX, the measured turbulent fluctuations are observed in the same k-space and exhibit density gradient drive consistent with TEM predictions from simulation. While the precise location of the measured fluctuations is unknown, measurements clearly establish that the changes observed occur in the region $r/a \leq 0.5$. As shown in Figs. 8(a) and (b), the density fluctuations increase with increasing density gradient scale length. If the fluctuations are more localized to r/a~0.5, scaling with density gradient suggest a critical gradient in the vicinity of $a/L_n \approx 2.5$, consistent with a Dimits shift possibly related to plasma flow. For r/a~0.3, the critical gradient would be much smaller. An upshift in the critical density gradient for TEM turbulence has been seen before in gyrokinetic simulations in the context of the tokamak [14] and is seen as a similar process to the Dimits shift observed in the case of ITG turbulence [15]. Present limitations of the fluctuation and equilibrium density profile measurements do not permit us to resolve this issue conclusively.

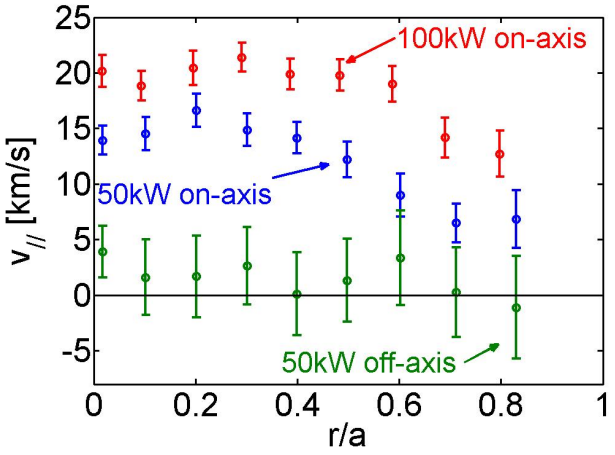

Figure 10. Plasma flow parallel to direction of symmetry measured by CHERS for 50kW with two heating locations: on-axis heating (blue) and HFS heating (green); and 100kW on-axis heating (red) for plasma with helical symmetry. [13]

The role played by plasma flow has yet to be explored in gyrokinetic simulations on HSX. The original goal of HSX was to experimentally validate the theoretical expectation of reduced neoclassical transport due to quasi-helical symmetry. However, there exists the possibility that improving neoclassical transport may also act to reduce turbulent transport. Mynick and Boozer [16] have modeled zonal flow response in stellarators and concluded that reductions in neoclassical transport, including those due to radial electric fields have reduced drift-polarization shielding and larger zonal flows. As with the tokamak case, the critical gradient shift can be attributed to the presence of strong zonal flows, which are known to moderate linear instabilities and reduce transport levels. Turbulence can be affected by both flow and flow shear but more detailed measurements and modeling are required to resolve the influence of this effect in HSX.

5. Conclusion

In this paper, the first density fluctuation measurements in the core of the HSX stellarator provide evidence for density gradient drive of broadband turbulence ($k_{\perp}\rho_s < 0.8$). No correlation between density turbulence and electron temperature gradient was observed. The measured density fluctuation characteristics, including frequency and wavenumber, are consistent with properties of TEM instabilities. For plasmas with reduced turbulence, the overall stored energy and global particle confinement were observed to increase while the global energy confinement was unchanged. In addition, changes in fluctuation amplitude with plasma flow also show a clear correlation supporting the thesis that increased flow may also act to reduce turbulence. Detailed comparison with gyro-kinetic simulation is required to unambiguously establish a causal connection between gradients, flows, confinement and fluctuation-induced transport. This will be the focus of future work on HSX where the GENE code will be employed to further characterize the plasma turbulence characteristics.

Acknowledgments

The authors would like to thank the entire HSX group for their contributions to and support of these investigations and Drs. W.X. Ding and J.N. Talmadge for helpful discussions. This material is based upon work supported by the U.S. Department of Energy Office of Science,

Office of Fusion Energy Sciences program under Award Numbers DE-FG03-01ER-54615 and DE-FG02-93ER54222.

References

[1] Yamada, H. for LHD experimental group, 2011 *Nucl. Fusion* **51,** 094021

[2] Hirsch, M. *et al* 2008 *Plasma Phys. Control. Fusion* **50,** 053001

[3] Yamada, H. *et al* 2001 *Nucl. Fusion* **41**, 901

[4] Canik, J.M. *et al* 2007 *Phys. Rev. Lett.* **98,** 085002

[5] Guttenfelder, W. *et al* 2008 *Phys. Rev. Lett.* **101**, 215002

[6] Weir, G. M. *et al* submitted to *Physics of Plasmas*

[7] Deng, C. B, Brower, D. L. *et al* 2009 *Phys. Rev. Lett.* **103**, 025003

[8] Deng, C. B, Brower, D. L. 2012 *Rev. Sci. Instrum.* **83**, 10E308

[9] Deng, C. B., Brower, D. L. 2010 *Rev. Sci. Instrum.* **81**, 10D503

[10] Ding, W. X, Brower, D. L. 2008 *Rev. Sci. Instrum.* **79**, 10E701

[11] Briesemeister, A., *et al* 2013 *Plasma Phys. Control. Fusion* **55**, 014002

[12] Zhai, K. *et al* 2004 *Rev. Sci. Instrum*. **75**, 3900

[13] Briesemeister, A. 2013 Thesis "*Measurement and Modeling of the Flows and Radial Electric Field in the HSX Stellarator*", University of Wisconsin-Madison

[14] Ernst, D. R. *et al* 2004 *Phys. Plasmas* **11**, 2637

[15] Dimits, A. M. *et al* 2000 *Nuclear Fusion* **40**, 661

[16] Mynick, H. E. and Boozer, A. H. 2007 *Phys. Plasmas* **14**, 072507